WELDING JOINT STRENGTH PROPERTIES FOR CRUCIFORM NATURAL FIBER COMPOSITES

J. Noda[1], T. Yamanaka[1], and S. Hamada[1]
[1] Department of Biomechanical and Human Factors Engineering, Kindai University, 930 Nishimitani, Kinokawa, Japan, nodaj@waka.kindai.ac.jp

Keywords: Joint, Cohesive element, Natural fiber composite, Finite elements, Crossbeam

ABSTRACT

Natural fiber composites (NFC) have several advantages in the development of tsunami shelters. First, they are carbon neutral, have low resource costs, and can be mass produced. In addition, NFC has excellent crashworthiness due to the high fracture strain of natural fibers. However, because NFC is derived from biomass, its long-term durability is an issue, and its general use has not grown as much as expected. Since this tsunami shelter is to be used only in an emergency, the durability of NFC is not a problem if it can be used for about one week. This is a practical example where the advantages of shelters that can be mass-produced and mass-installed at low cost can be utilized. To develop a low-cost, high-strength tsunami shelter, we proposed a hemispherical crossbeam structure with unidirectional NFC tapes. Off-axis compression analysis and progressive compression tests were conducted on the hemispherical crossbeam structure. The results showed that the occurrence of delamination between crossbeams leads to the failure of the entire structure. In this study, focusing on the stacking method of the crossbeam structure, an out-of-plane delamination test was proposed and conducted using cross-shaped specimens formed by thermally bonding unidirectional NFC tape to investigate the effect of different stacking order on strength properties. In addition, delamination analysis using the cohesive zone model (CZM) at the adhesive interface of the cross-shaped specimens was conducted. By comparing the analysis results, the validity of the proposed test method was confirmed.

1 INTRODUCTION

In the event of a tsunami caused by an earthquake, it is effective to evacuate to the nearest high ground. If no high ground is available, temporary evacuation facilities such as tsunami shelters are effective. Tsunami shelters must be unsinkable, have high specific elastic modulus, high strength, and impact resistance, and some are made of short fiber FRP. FRP is well known for its high specific elastic modulus and strength, but it is difficult to form angular shapes with long fibers. In order to form three-dimensional spherical structures such as tsunami shelters using long fiber-reinforced composites with high specific strength, it is necessary to develop crossbeam structures. On the other hand, although much research has been conducted in various fields on FRP recycling [1,2], most of the FRP is currently disposed of in landfills due to the high cost of separating the fibers from the resin. Therefore, the practical application of natural fiber composites (NFC) is attracting attention in order to realize a sustainable society. NFC has several advantages in the development of tsunami shelters. First, it is carbon neutral and inexpensive in terms of resources required for mass production. In addition, NFC has excellent crashworthiness due to the high breaking strain of natural fibers. However, because NFC is derived from biomass, its long-term durability is an issue, and its general use has not grown as much as expected. Since this tsunami shelter will be used only in an emergency, the durability of NFC is not a problem for a one-week period of use. This is a practical example where the advantages of low-cost, mass-produced and mass-installed shelters can be utilized. To develop a low-cost, high-strength tsunami shelter, we proposed a hemispherical crossbeam structure with unidirectional NFC tape [3]. The concept of the proposed tsunami shelter is shown in Figure 1.

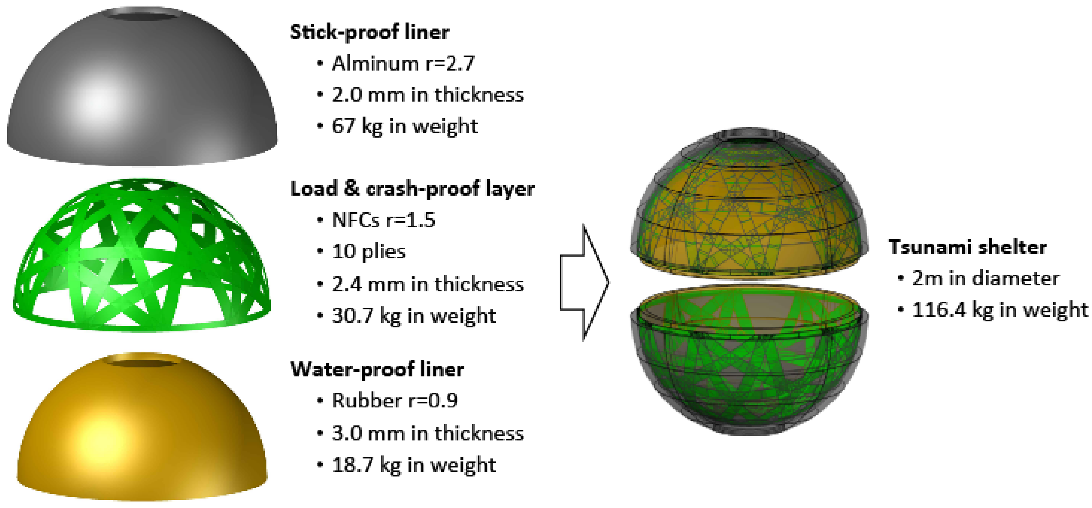

Figure 1: Proposed tsunami shelter concept

Off-axis compression analysis and progressive compression tests were performed on the hemispherical crossbeam structure. Typical off-axis compression analysis results and laboratory-scale compression test results are shown in Figure 2. The results indicate that the occurrence of delamination between crossbeams leads to failure of the entire structure; C. Blondeau et al [4] conducted DCB tests, a Mode I interlaminar fracture toughness test method, at the interface of three types of inversely symmetrical CFRP laminates to investigate the effect of orientation angle on crack propagation resistance. The results showed that the fracture resistance of the angle-ply interface was much stronger than that of the unidirectional laminate, but unstable crack propagation occurred, as observed in their study. These findings may be applicable to delamination phenomena in crossbeam joints, since the direction of loading and the direction of crack propagation are different.

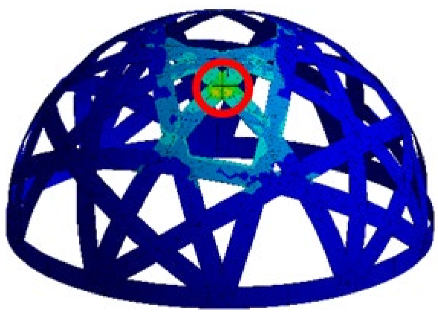

(a) Equivalent stress distribution

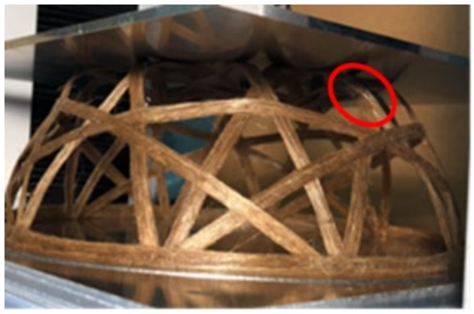

(b) Progressive compressive test

Figure 2: Finite element analysis and compression test for laboratory-scale compression test

In this study, focusing on the stacking method of the cross beam structure, we proposed and conducted an out-of-plane peel test using cross-shaped specimens formed by thermally bonding unidirectional NFC tapes in order to investigate the effect of different stacking order on strength properties. In addition, a peel analysis using a cohesive zone model (CZM) at the adhesive interface of the cross-shaped specimen was conducted. By comparing the analysis results, the validity of the proposed test method was confirmed.

2 OUT-OF-PLANE DELAMINATION

2.1 Material and specimens

Out-of-plane delamination tests with Mode I (out-of-plane direction) crack propagation were conducted using a cruciform specimen as the basic geometry and failure mode. First, a cruciform specimen was prepared by intersecting unidirectional tapes. Here, a cruciform specimen with three unidirectional tapes stacked on top of each other (3+3 specimen) and a cruciform specimen with six tapes alternating one on top of the other ((1+1)x3 specimen) were prepared. These cruciform specimens were preformed by cutting FLAXPREG T-UD PP tape (CAP SEINE FLAX UNIT, France), crossing it in a crossbeam, covering it with a backing film, and heating it in an oven at 200°C for 20 minutes under vacuum as shown in Figure 3. The crossbeams were 160 mm long and 10 mm wide. The thickness was 1.05 mm. Next, a new out-of-plane delamination test fixture was designed and fabricated from steel. The cruciform specimen and jig were mounted on a small tabletop testing machine as shown in Fig. 3.

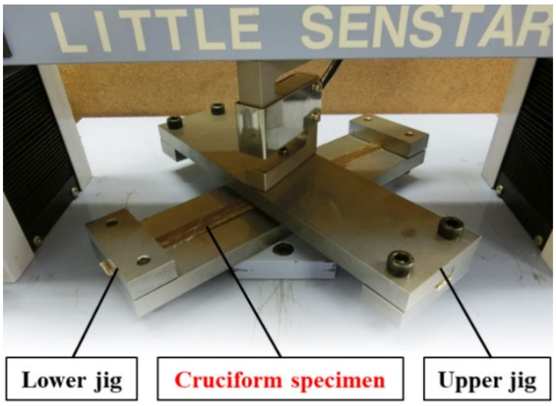

Figure 4: Out-of-plane delamination test setup

2.2 3+3 cruciform specimens

As a result of out-of-plane delamination tests, delamination was observed at the intersection of the crossbeams. Fiber bridging was observed on the delaminated surface, and the cruciform specimens, which were welded together at a pressure of about vacuum pressure assistance, were bonded quite tightly. The relationship between the load and stroke of the out-of-plane delamination test is shown in Fig. 5. Fig. 5 also shows the deformation of the cruciform specimen observed from a 45-degree angle in the plane. From this figure, it was clear that the specimen exhibits the following three deformation and fracture phases. First, (a) the load increased in the bending mode in which the upper and lower pairs of three-point bending deformations were dominant. Next, (b) the load shifted to the four-crossbeam tensile mode after the stroke exceeded 8 mm. Finally, (c) delamination started and the final separation occurred.

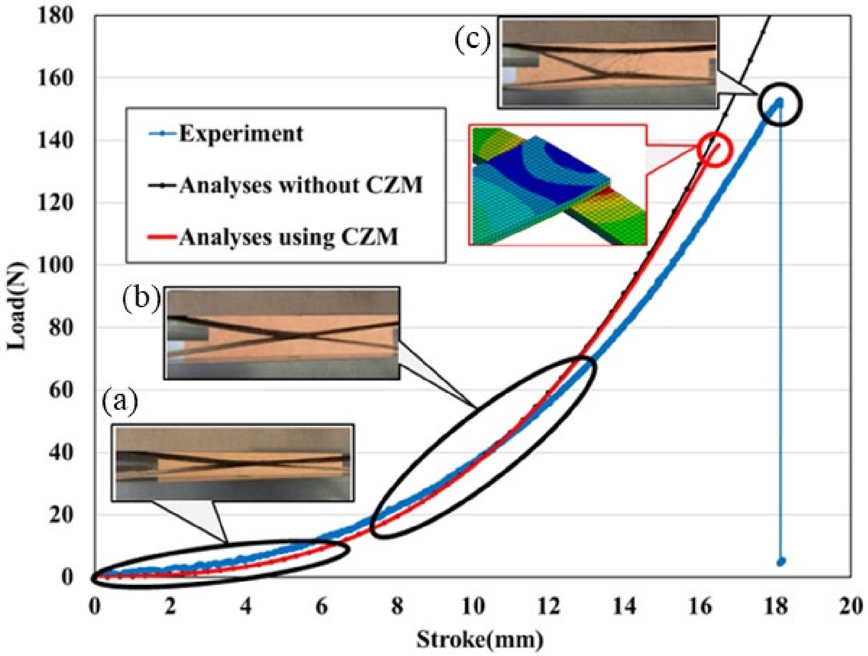

Figure 5: Load-stroke diagrams of Mode I delamination tests using 3+3 cruciform specimens

2.3 (1+1)x3 cruciform specimens

The relationship between the load and stroke of the out-of-plane delamination test is shown in Fig.6. Fig. 6 also shows the deformation of the cruciform specimen observed from a 45-degree angle in the plane. This figure shows that the maximum load was higher for the alternately stacked specimens than those for the 3+3 specimens. No delamination occurred and the load shifted to the four-crossbeam tensile mode after the stroke exceeded 12 mm.

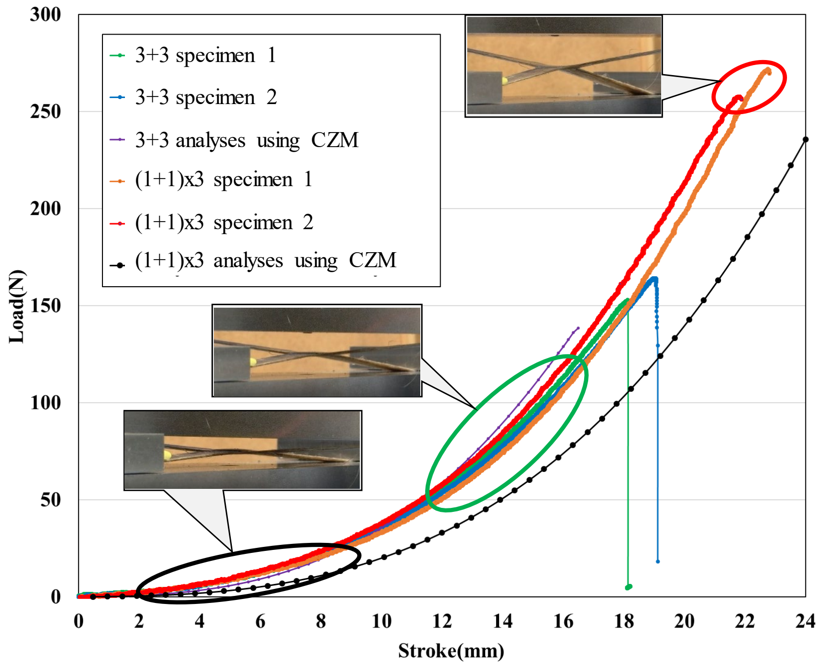

Figure 6: Load-stroke diagrams of Mode I delamination tests using (1+1)x3 cruciform specimens

2.4 Finite element analyses for out-of-plane delamination using cohesive elements

A finite element model for out-of-plane delamination using CZM was conducted to investigate the interface delamination conditions at the joint of cruciform specimens. The finite element model was shown in Fig. 7. Workbench of ANSYS version 19.1 was used as the solver. An auto-mesh was performed using hexahedral 20-node solid elements, and the aspect ratio of the elements ranged from 1.04 to 1.07, with an average of 1.05. The boundary conditions were as follows. The symmetry of the shape of the cruciform specimen was used to fabricate a half model. The thickness was set to 1.05 mm assuming a three-ply laminate, and orthotropic anisotropy was introduced into the crossbeam. The material properties of the assumed flax fiber/PP composite tape are shown in Table 1. Based on the test results, the CZM parameters fitted in the analysis were Mode I traction force T_I of 20 MPa and Mode I cohesive energy dissipation G_{IC} of 1000 J/m^2. The number of nodes in the 3+3 model was 20,736 and the number of elements was 12,800. In order to confirm the validity of CZM, the analysis was also conducted with the same boundary conditions by constructing shared nodes without using the cohesive elements.

The load-stroke relationships for the analysis results with CZM and without CZM were appended in Fig. 5 and 6. By fitting the experimental results with CZM parameters, the delamination phenomenon could be simulated in the analysis. It was confirmed that the load-bearing capacity increased significantly by switching from 3+3 lamination to alternating lamination. The increase in load capacity is thought to be due to a change in failure mode from delamination to fiber failure.

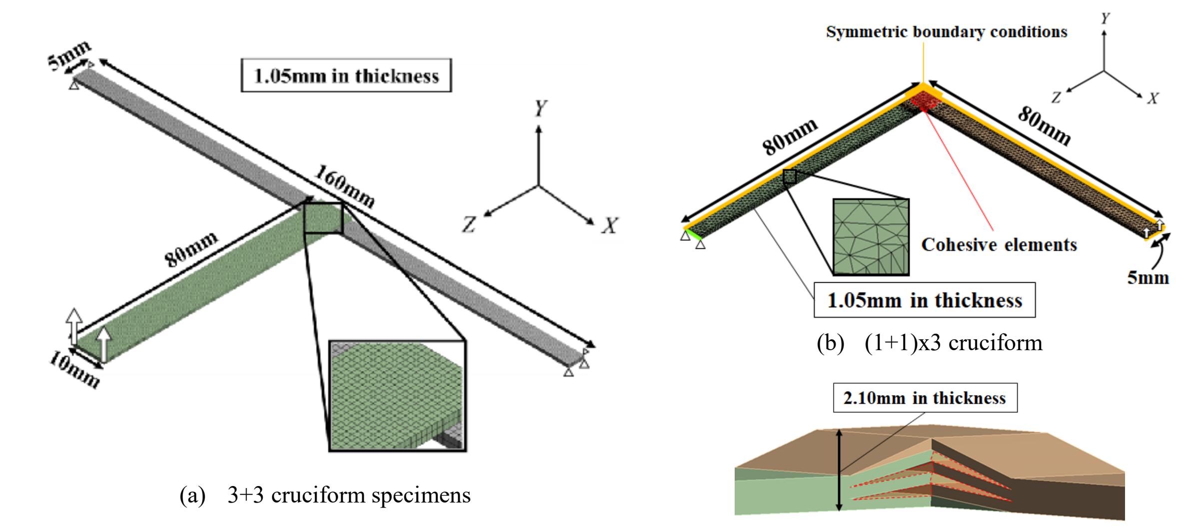

(c) FE model at joint

Figure 7: FE model and boundary conditions for out-of- plane delamination model

Table 1: Material properties of flax/PP for FEM analysis

Longitudinal elastic modulus E_L [GPa]	Transverse elastic modulus E_T [GPa]	Poison's ratio ν_{LT} [-]	Poison's ratio ν_{TT} [-]	Shear modulus G_{LT} [GPa]	Shear modulus G_{TT} [GPa]
20.0	1.79	0.0261	0.442	1.432	1.074

3 IN-PLANE SHEAR DELAMINATION

3.1 Cruciform specimen and jig for in-plane delamination test

Since not only Mode I but also Mode II delamination has a significant influence on the failure of crossbeam joints in GC domes, CZM parameters (tractions and cohesive energy dissipations) for Mode II delamination propagation must also be identified. To simulate Mode II crack-dominated delamination, a novel test jig was fabricated to prevent out-of-plane bending and torsion of the cruciform specimens. Fig. 8 shows the in-plane shear type delamination test jig with a restrained cruciform specimen mounted on a small table-top testing machine. The cruciform specimen has a crossbeam length of 200 mm, a width of 20 mm, and a thickness of 2.1 mm. Thin aluminum foil with a thickness of 11 μm was formed between the corners of the joint interface to introduce a pre-crack and stabilize crack propagation. In addition, a cruciform specimen with a circular hole of 10 mm in diameter was also introduced to examine the effect of friction at the center of the bonding interface, and delamination tests were conducted.

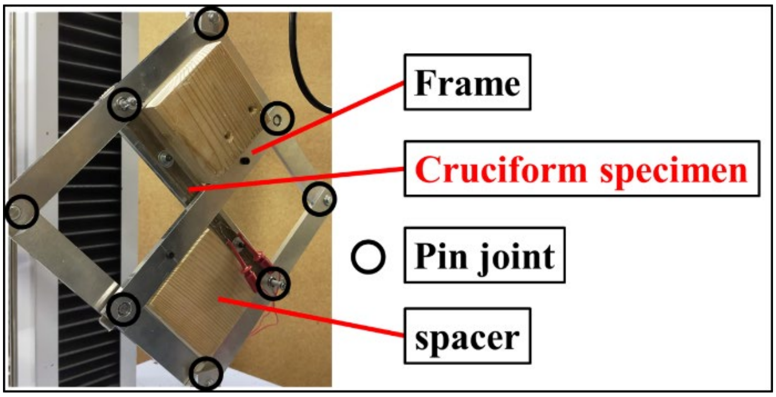

Figure 8: In-plane shear delamination test setup

3.2 Finite element analyses for in-plane delamination using cohesive elements

A finite element model for in-plane delamination using CZM was conducted to investigate the interface delamination conditions at the joint of cruciform specimens. The finite element model was shown in Fig.9. These analyses were performed to validate the proposed test method and identify CZM parameters. Auto-mesh was performed using rigid and shell elements, and the aspect ratio of the elements ranged from 1.0~4.5, with an average of 1.1. The model had 4,441 nodes and 4,007 elements. The boundary conditions were set so that the pin joints were free to rotate, and the out-of-plane deformation was suppressed by constraining the out-of-plane direction of the cruciform specimen section. The CZM parameters fitted in the analysis were a Mode II traction force T_{II} of 2 MPa and a Mode II cohesive energy dissipation G_{IIC} of 200 J/m^2. The in-plane delamination analyses and experimental results with and without a 10 mm diameter circular hole were shown in Fig. 10, respectively.

Fig.11 shows the Mode II maximum stress distribution and the associated slip. Although the initial slopes of the two modes agree well, a 116% difference in load is observed due to interfacial friction after debonding in the comparison without the circular hole in the black line. Fracture toughness due to friction occurred in the black area because friction was not considered in the analysis because it is extremely difficult to simulate friction between interfaces after the damage initiation criterion is satisfied and bond strength is completely lost in a CZM analysis. In comparison, the red comparison with circular holes showed that the difference was suppressed to 27.5%, but the load gradient was maintained due to friction. However, the fitted Mode II maximum bond strength and fracture toughness values are reasonable because they simulate Mode II crack-dominated debonding in the early loading phase. Therefore, the validity of the test method and analysis proposed in this study was demonstrated. In this study, circular holes were drilled to remove the effects of friction and bridging, but the improved fracture toughness is expected to be effective in practical use.

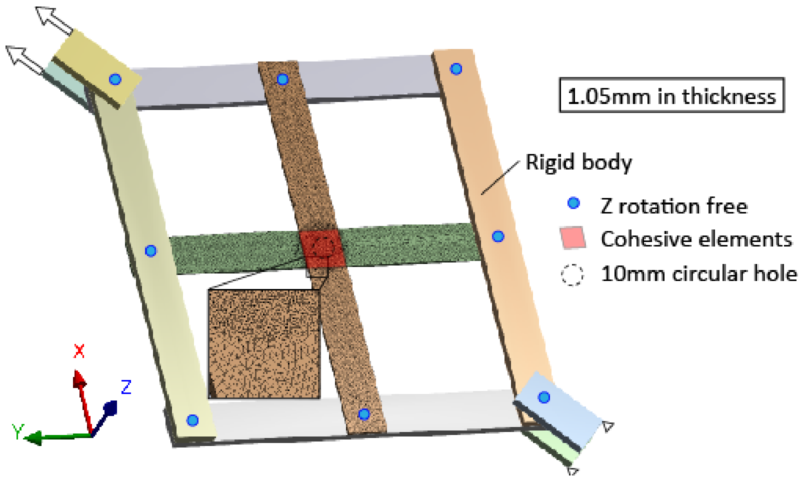

Figure 9: FE model and boundary conditions for in-plane delamination model

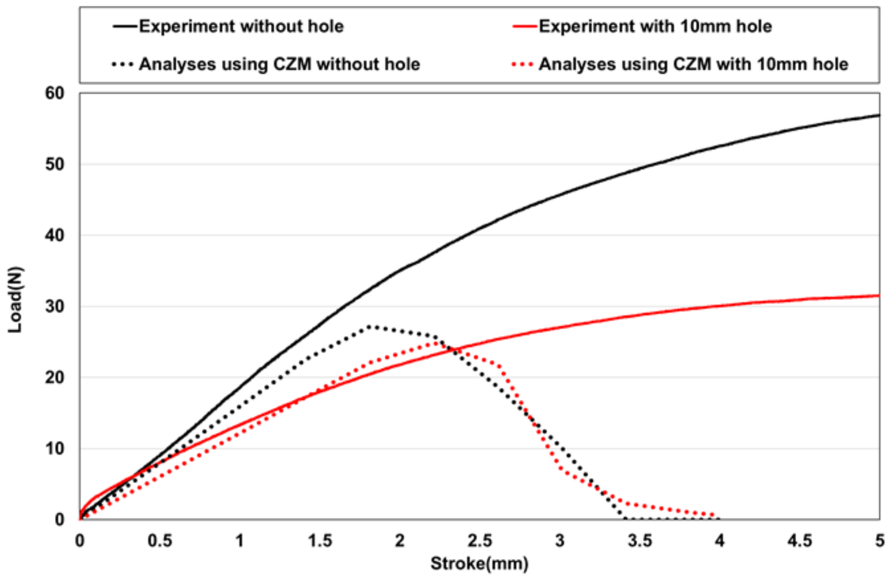

Figure 10: Load-stroke diagrams of in-plane delamination tests using cruciform specimens

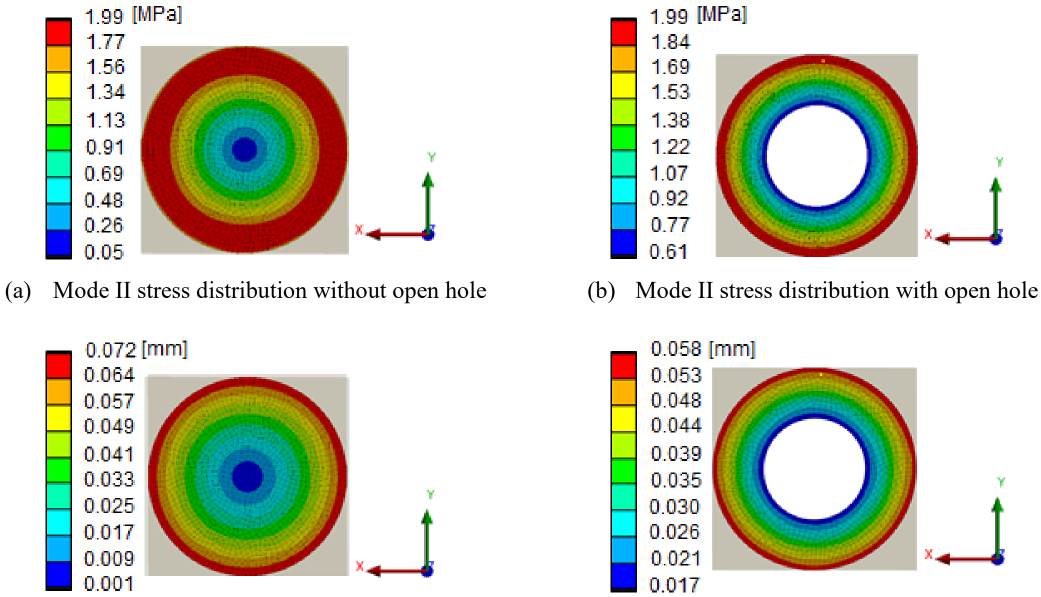

(c) Sliding distance without open hole (d) Sliding distance with open hole

Figure 11: Mode II stress content and its sliding distance distributions

4 CONCLUSIONS

In this study, out-of-plane delamination tests and in-plane shear delamination tests using cruciform specimens were conducted to experimentally verify the fracture behavior. The validity of the proposed delamination test method and analysis was examined by performing a delamination analysis using CZM and comparing it with the test results. As a result, the following were found.

1. The load-bearing capacity increased significantly by switching from 3+3 lamination to alternating lamination. The increase in load capacity is thought to be due to a change in failure mode from delamination to fiber failure.
2. By comparing the out-of-plane delamination test results with the CZM analysis, the out-of-plane delamination behavior could be simulated by fitting the traction force and cohesive energy dissipation for Mode I.
3. In in-plane shear delamination tests, the introduction of a pre-crack at the edge of the welded-joint interface of a cruciform specimen was effective because it stabilizes crack propagation and reduces the initial slope variation.
4. Fiber bridging and friction continue to occur at the delaminated interface, causing the load gradient to increase even after delamination. This increase in load due to interfacial friction after delamination could be suppressed by opening a circular hole in the center of the bonding interface.
5. By constraining the out-of-plane deformation and simulating Mode II crack-dominated delamination in the initial loading phase, the CZM parameters, i.e., Mode II traction force and cohesive energy dissipation, could be identified.

ACKNOWLEDGEMENTS

This work was supported by JSPS KAKENHI Grant Number JP21K03760.

REFERENCES

[1] H. Hanaoka, H. Ikematsu, S. Takahashi, N. Ito, N. Ijuin, H. Kawada, Y. Arao and M. Kubouchi, Recovery of carbon fiber from prepreg using nitric acid and evaluation of recycled CFRP, *Composites Part B*, **231**, 2022, 109560.

[2] A.D.L. Rosa, S. Greco, C. Tosto and G. Cicala, LCA and LCC of a chemical recycling process of waste CF-thermoset composites for the production of novel CF-thermoplastic composites, Open loop and closed loop scenarios. *Journal of Cleaner Production*, **304**, 2021, pp. 127-158.

[3] J. Noda, T. Yamanaka and T. Miyamoto, Development of tsunami shelter structure using green composites, *Proceedings of 1st Russia-Japan Joint workshop on composite materials, Moscow, Russia*, 2019, IS12.

[4] C. Blondeau, G. Pappas and J. Botsis, Influence of ply-angle on fracture in antisymmetric interfaces of CFRP laminates, *Composite Structures*, **216**, 15, 2019, pp.464-476.